SEMI-INCLUSIVE DEEP INELASTIC SCATTERING

M. DÜREN

Univ. Erlangen-Nürnberg, Erwin-Rommel-Str. 1, 91058 Erlangen, Germany

Semi-inclusive deep inelastic scattering experiments provide important information about the quark and gluon structure of the nucleon. The knowledge of the fragmentation process is used to measure quark distributions separately for various flavors. The light quark sea shows a large enhancement of $\bar{d}$-quarks compared to $\bar{u}$-quarks. The polarization of up quarks in the valence region is large and positive, the polarization of down quarks is negative. The polarization of the quark sea is compatible with zero. At HERA collider energies the tagging of leading baryons allows to select events where the virtual photon couples to virtual pions which appear in the proton. The process is used to extract deep inelastic pion structure functions.

1 Motivation

Semi-inclusive deep inelastic scattering (DIS) is an ideal experimental method to study properties of quarks in nucleons and nuclei. In Born approximation the scattering process is described by the exchange of a virtual photon which couples to a quark inside the nucleon as illustrated in Figure 1. The energy $E(E')$ of the incoming (scattered) lepton and its scattering angle θ are measured and thus the momentu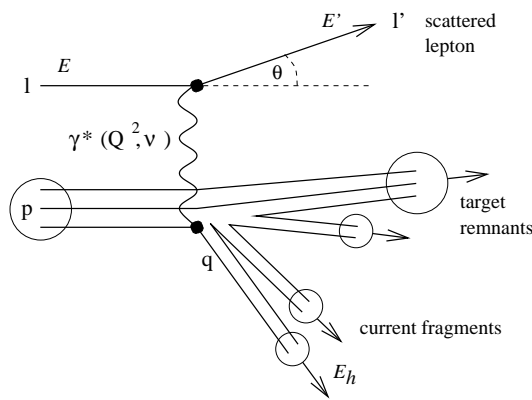m transfer to the struck quark is experimentally determined. The kinematic quantity $Q^2 = 4EE'\sin^2\theta/2$ is related to the resolution of the virtual photon. To be able to 'see' the quark structure of the nucleon, Q^2 should be larger than about 1 GeV^2. Other important quantities are the energy transfer $\nu = E - E'$ to the quark and the 'momentum fraction' $x = Q^2/2M\nu$ of the quark in the nucleon, where M denotes the mass of the nucleon. All definitions are

Figure 1. The kinematic diagram of semi-inclusive deep inelastic scattering.

given in the rest frame of the nucleon. Collider kinematics differ by a Lorentz transformation of the lepton kinematic variables E, E', θ. In an experiment with polarized beam and target, not only the momentum transfer but also the spin transfer of the photon to the quark is known and the quark spin can be related to the spin of the target nucleon.

Semi-inclusive DIS is characterized by the observation of the final state hadrons in addition to the scattered lepton. This allows to test basic ingredients of the quark model, like the factorization of the process into a quark scattering and a fragmentation part. The basic kinematic variable is the energy fraction $z = E_h/\nu$ of the hadron after fragmentation. Here E_h is the energy of the hadron in the rest frame of the nucleon. The Feynman scaling variable $x_F \approx 2p_L/W$ is the longitudinal 'momentum fraction' of the hadron in the center of mass system of the hadronic final state with mass $W = \sqrt{M^2 + 2M\nu - Q^2}$. x_F is positive for particles that are related to the struck quark and negative for particles of the target remnant. Even at lower energies, where factorization of scattering and fragmentation does not apply completely, the observation of the leading hadrons in the current region allows to determine with a certain statistical confidence the flavor of the struck quark. This way semi-inclusive DIS can be used to determine spin and momentum distributions separately for each quark flavor.

At high energies a jet is generated which coincides with the (experimentally determined) direction of the struck quark. At HERA energies a phenomenon called *rapidity gaps* has been observed[1,2] which points to an interaction beyond the simple scattering picture from Figure 1.

2   Experiments

A common requirement for semi-inclusive DIS experiments is the ability to measure the scattered lepton in coincidence with the final state hadrons. An excellent example is the NA9 experiment of EMC[3] which had an almost complete acceptance of the hadronic final state. Table 1 summarizes the main properties of the recent experiments which are mentioned in this paper. Experiments with unpolarized semi-inclusive DIS physics are at Fermilab the E665 experiment, and at HERA the collider experiments H1 and ZEUS and the fixed target experiment HERMES[4]. The collider experiments are the high energy frontier and cover the very low $x > 10^{-6}$ and the very high $Q^2 < 3.5 \cdot 10^4$ GeV^2 range. Due to its large beam energy, SMC covers data at lower x ($x > 0.003$) than other spin experiments. The advantages of HERMES are the pure polarized targets and the good particle identification. HERMES makes use of two rather novel experimental techniques: spin

Table 1. Beam energies and target types of semi-inclusive DIS experiments.

EXPERIMENT	BEAM		TARGET	
Unpolarized:				
E665 (Fermilab)	470 GeV	μ	H, ...	fixed target
H1, ZEUS (DESY)	27 GeV	$e^{\pm}$	820/920 GeV p	collider
HERMES (DESY)	27 GeV	$e^{\pm}$	H, D, ^{3}He, N, Kr	fixed targets
Polarized:				
SMC (CERN)	190 GeV	μ	H, D (buthanol)	solid targets
HERMES (DESY)	27 GeV	$e^{\pm}$	H, D, ^{3}He	gas targets

rotators turn the spin of the transversely polarized positrons in the HERA ring into longitudinal direction at the HERMES target region[5]. A storage cell confines the atoms from a polarized or unpolarized source in the region of the HERA electron beam and increases the density of the target by a factor of about 100. A target thickness of $10^{14(15)}$ nucleons/cm^2 can be achieved for polarized H (^{3}He).

3 Fragmentation

Due to confinement, a quark which is kicked out of a nucleon fragments into hadrons. This can be described by the phenomenological fragmentation functions $D_f^h(z)$ which are a measure of the probability that a hadron h with the energy fraction z is produced from a quark with flavor f[6,7]. The differential cross section $d\sigma^h$ for producing a hadron of type h is given as

$$\frac{d\sigma^h(z, x, Q^2)}{dz} = \frac{\sum_f e_f^2 q_f(x, Q^2) D_f^h(z)}{\sum_f e_f^2 q_f(x, Q^2)} \sigma^T(x, Q^2), \tag{1}$$

where $\sigma^T(x, Q^2)$ is the total (inclusive) cross section. The formula assumes that the quark scattering process and the fragmentation process factorize and that the fragmentation functions scale and only depend on the fractional energy z. Both assumptions are experimentally confirmed to a certain level[3,8]. The number of different fragmentation functions which describe the production of charged pions on proton and neutron targets can be reduced to three by applying charge and isospin symmetries. $D^+(z)$ ($D^-(z)$) is called the favored (unfavored) fragmentation function and describes the production of pions which contain (do not contain) the struck quark. $D_s(z)$ describes the production of pions from strange quarks. Certainly, the reduction to three fragmentation functions is only approximately valid and cannot be applied

to the target fragmentation region as the production of e.g. a π^+ from a proton remnant will not be identical to the production of a π^+ from a neutron remnant. Therefore at low W, where the current and target fragmentation regions overlap, three fragmentation functions are not sufficient. Figure 2 shows the favored and unfavored fragmentation functions as measured
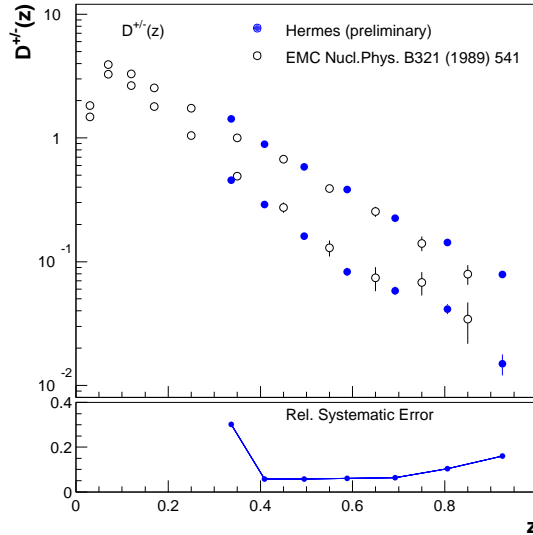

by HERMES[9] and EMC. Both results agree within their uncertainties although the beam energy of the experiments differs by a factor of 10. The small difference between the two experiments might be due to a small Q^2 dependence of the fragmentation functions. An evaluation of data from experiments at higher energy (E665, H1, ZEUS)[10] shows that there is a small but significant Q^2 and W^2 dependence in the fragmentation distributions. These dependencies are reproduced by standard fragmentation models based on QCD and color strings or parton showers[10].

Figure 2. The fragmentation functions D^+ (upper points) and D^- (lower points) as a function of the energy fraction z.

3.1 Hadronization in Nuclei

The comparison of fragmentation distributions in various nuclei is of special interest as it allows to measure the space-time structure of the hadronization process. This is illustrated in the sketch below: It takes a certain time for the struck quark to form a hadron. At low ν the formation takes place inside the nucleon and an attenuation of the production of hadrons in a large nucleus compared to a small nucleus is observed. At large ν, due to the large Lorentz boost, the forma-
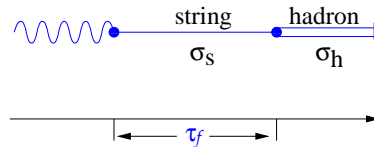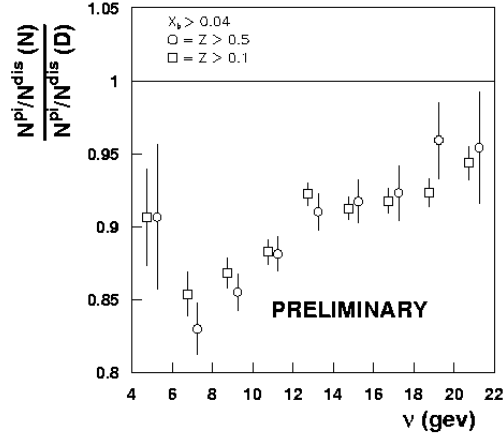
Figure 3. The ratio of hadron multiplicities in nitrogen compared to deuterium.

tion distance becomes larger, takes place outside the nucleus and as a result the hadron production becomes independent of the size of the nucleus. This effect has been seen recently on a nitrogen compared to a deuterium nucleus in the HERMES experiment[11] in a dedicated high luminosity run with $\mathcal{L} \sim 10^{33}\text{atoms/cm}^2/\text{s}$. The result as shown in Figure 3 demonstrates that HERMES is just in the interesting energy range. More data on different nuclei are needed for a more detailed understanding of the hadronization process.

3.2 Rapidity Gaps and Leading Baryons

By studying the energy flow of DIS events at high energies, H1 and ZEUS observed an excess of events with large 'rapidity gaps', i.e. events without hadrons in a region between the current and the target jet[1,2]. This observation questioned the assumption that there is always a color string between the struck quark and the target remnant which would lead to a continuous rapidity distribution in the hadron production. A natural explanation for this observation is that in rapidity gap events the DIS process takes place off a colorless object which is distinct from the target proton. This object is identified as a pomeron, reggeon or simply a pion. As a consequence of this picture, the target proton should appear after the interaction as a high energy, forward going baryon with small transverse momentum.

The H1 and ZEUS detectors both include a leading proton spectrometer and a forward neutron calorimeter which were build to detect target baryons. Indeed it was found that about 15% of the DIS events had a leading baryon with a fractional energy of $0.5 < x_L < 0.95$[12]. The fraction of leading baryon events turned out to be approximately constant over several orders of magnitude in x and Q^2. In the 'exchange picture' the observation of a leading neutron is described by a cross section which factorizes into the flux of pions

in the proton $f_{\pi/p}$ and the DIS cross section of the pion $\sigma(e\pi \to e'X)$:

$$\sigma(ep \to e'NX) = f_{\pi/p}(x_L, p_t^2)\sigma(e\pi \to e'X). \qquad (2)$$

Under the assumption of an approximately constant pion flux factor of 0.131, the HERA data can be used to extract the pion structure function. First results were extracted by H1 as shown in Figure 4[13].
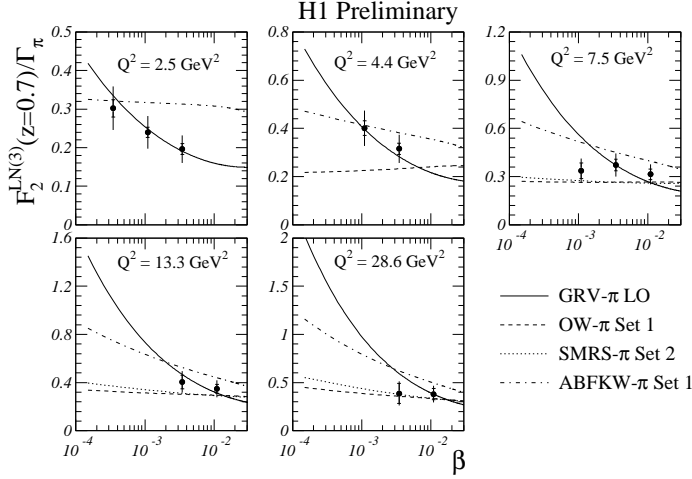

Figure 4. In the 'exchange picture', the pion structure function F_2^π is equivalent to the ratio of the leading neutron structure function $F_2^{LN(3)}$ and the pion flux factor Γ_π. The data are compared to various parameterizations of F_2^π.

4   Quark Flavor Tagging

The idea of flavor tagging is to reconstruct the flavor of the struck quark from the observed hadron types. Roughly speaking one expects on a proton target predominantly positive pions from up quarks, negative pions from down quarks and negative kaons from strange quarks. On a neutron target the isospin inverted quark distributions are selected. A useful quantity for the

extraction of the quark flavor distributions is the 'purity'

$$P_f^h(x, Q^2) = \frac{e_f^2 q_f(x, Q^2) \int_{0.2}^1 D_f^h(z, Q^2)\, dz}{\sum_{f'} e_{f'}^2 q_{f'}(x, Q^2) \int_{0.2}^1 D_{f'}^h(z', Q^2)\, dz'} \tag{3}$$

which denotes a probability that a given hadron h originated from a quark of flavor f[14]. These purities can be directly calculated from measured fragmentation functions or can be extracted by Monte Carlo methods from a given fragmentation model.

4.1 Flavor Asymmetry of the Light Sea

The flavor content of the light quark sea has come to be recognized as an important domain for testing models of the nucleon structure[15]. The assumption, that due to flavor blindness of QCD the light quark sea is symmetric was questioned by the observation of NMC that the Gottfried Sum rule is violated[16]. The flavor tagging method in semi-inclusive DIS was applied by HERMES to extract the flavor content of the sea. The following combination of positive (negative) pion yields $N^{\pi^{+(-)}}$:

$$\frac{N_p^{\pi^-} - N_n^{\pi^-} + N_p^{\pi^+} - N_n^{\pi^+}}{N_p^{\pi^+} - N_n^{\pi^+} - N_p^{\pi^-} + N_n^{\pi^-}} = \frac{3}{5} \cdot \frac{\tau(x) - \bar{\tau}(x)}{\tau(x) + \bar{\tau}(x)} \cdot \frac{D^+(z) + D^-(z)}{D^+(z) - D^-(z)} \tag{4}$$

with $\tau(x) = u(x) - d(x)$ and $\bar{\tau}(x) = \bar{d}(x) - \bar{u}(x)$ is used to extract the flavor asymmetry. The right hand side of the equation factorizes into an x and a z dependent part. The left plot in Figure 5 demonstrates that factorization holds in the kinematic range of HERMES, at least within the statistical precision of this experiment. The extracted flavor asymmetry is independent of the hadron variable z. The right plot in Figure 5 shows the result from HERMES[17] as function of x compared with recent data from the Drell-Yan experiment E866[18]. There is a large significant excess of $\bar{d}$ over $\bar{u}$ at low x ($x < 0.2$). The two experiments give consistent values for $\bar{d} - \bar{u}$ even though the average Q^2 differs by about a factor of 20. Pertubative QCD calculations cannot account for this asymmetry as the color forces are flavor independent and as the confinement scale is much larger than the differences of the quark masses which are involved. There are many models which try to explain the asymmetry[19,20]. Figure 6 sketches the nucleon-'pion' model and the chiral quark model where in both cases an excess of virtual π^+ is responsible for the enhanced $\bar{d}$ content of the sea. E866 fitted their pion model to the $\bar{d}(x)/\bar{u}(x)$ data with the conclusion that the proton is for $(20 \pm 4)\%$ of the time in a pion-nucleon state and for $(10 \pm 2)\%$ in a pion-delta state[18].
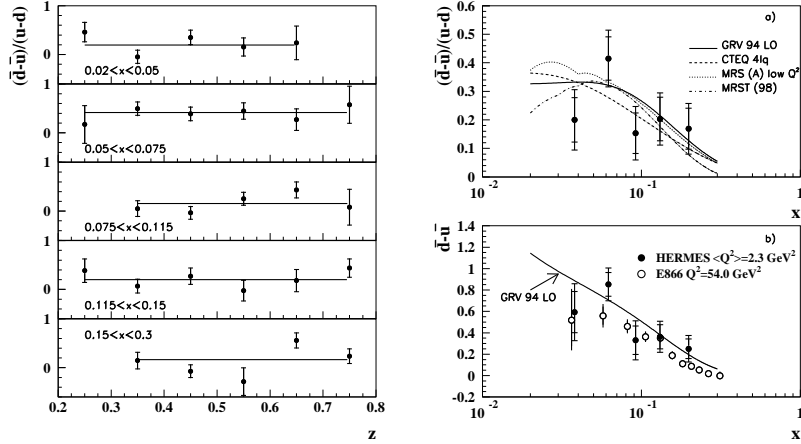
Figure 5. The left plot proves that the extracted flavor asymmetry from HERMES is independent of the hadron variable z. The right figure shows the results for the flavor asymmetry as function of x for HERMES data, E866 data and various parameterizations.
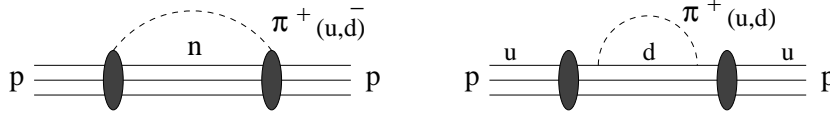

Figure 6. The nucleon-'pion' model (left) and the chiral quark model (right) both explain the enhancement of $\bar{d}$ by an enhanced occurrence of virtual π^+.

4.2 Flavor Decomposition of Polarized Quark Distributions

The understanding of the spin structure of the nucleon in terms of quarks and gluons remains a challenge since it was demonstrated by EMC[21] and later experiments using inclusive DIS, that only a small fraction of the nucleon spin can be attributed to the quark spin. Semi-inclusive polarized DIS experiments are able to measure the separate spin contributions Δq_f of quark and anti-quark flavors f to the total spin of the nucleon, as a function of the Bjorken scaling variable x. Inclusive experiments are not able to separate flavor distributions and can only extract first moments of up, down and strange quark spin distributions by assuming $SU(3)_f$ flavor symmetry. This kind of

analysis lead to the conclusion that the spin of the quarks contributes only little to the total spin of the nucleon and that the strange quark sea seems to be negatively polarized[22]. Semi-inclusive data can be used to measure the sea polarization directly and to test the $SU(3)_f$ symmetry.

It is assumed that the fragmentation process is spin independent, i.e. that the probability to produce a hadron of type h from a quark of flavor f is independent of the relative spin orientations of quark and nucleon. The spin asymmetry A_1^h in the semi-inclusive cross section for production of a hadron of type h by a polarized virtual photon is given by

$$A_1^h(x, Q^2, z) = \frac{\sum_f e_f^2 \Delta q_f(x, Q^2) D_f^h(z, Q^2)}{\sum_f e_f^2 q_f(x, Q^2) D_f^h(z, Q^2)} (1 + R(x, Q^2)) \tag{5}$$

where $\Delta q_f(x, Q^2) = q_f^+(x, Q^2) - q_f^-(x, Q^2)$ is the polarized quark distribution function and $q_f^{+(-)}(x, Q^2)$ is the distribution function of quarks with spin orientation parallel (anti-parallel) to the spin of the nucleon. The ratio $R = \sigma_L/\sigma_T$ of the longitudinal to transverse photon absorption cross sections appears in this formula to correct for the longitudinal component that is included in the experimentally determined parameterizations of $q_f(x, Q^2)$ but not in $\Delta q_f(x, Q^2)$. It is assumed that the ratio of longitudinal to transverse components is flavor and target independent. Equation (5) is used to extract the quark polarizations $\Delta q_f(x)/q_f(x)$ from a set of measured asymmetries on the proton and neutron for positively and negatively charged hadrons.

Figure 7 shows results of the purity analyses from SMC[23] and HERMES[24] for the valence and sea quark spin distributions. Both data sets agree within their systematic uncertainties. To reduce the number of degrees of freedom in the flavor
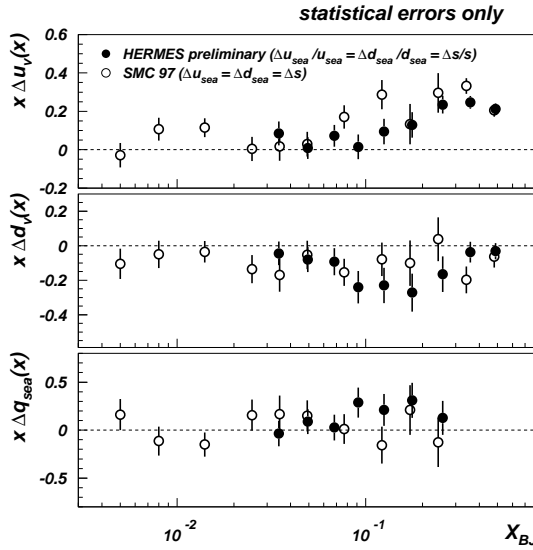

Figure 7. The valence and sea quark spin distributions from SMC and HERMES.

decomposition, both experiments make certain assumptions about the sea. SMC assumes a flavor symmetric spin distribution $\Delta u_s = \Delta d_s = \Delta s = \Delta \bar{u} = \Delta \bar{d} = \Delta \bar{s}$ whereas HERMES assumes a flavor symmetric polarization $\frac{\Delta u_s}{u_s} = \frac{\Delta d_s}{d_s} = \frac{\Delta s}{s} = \frac{\Delta \bar{u}}{\bar{u}} = \frac{\Delta \bar{d}}{\bar{d}} = \frac{\Delta \bar{s}}{\bar{s}}$. Figure 8 shows the flavor decomposition of the quark spin into up and down polarizations from HERMES data. At small x the polarization of the quarks is small. At large x the polarization of the up quarks is large, above 50%, whereas the polarization of the down quarks is negative and on the order of up to 30%. The data agree within the systematic uncertainties with various parameterizations of the parton distributions. The different sets shown correspond to the following authors: *Set 1*: Bartelski and Tartur[25] (LST(15)=105), *Set 2*: Gehrmann and Stirling[26] ('Gluon A' (LO), LST(15)=110) and *Set 3*: Glück et al.[27] ('standard scenario' (LO), LST(15)=118).
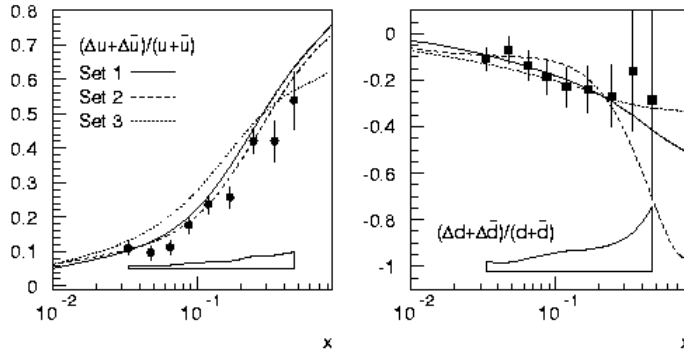

Figure 8. The quark flavor polarizations $(\Delta u + \Delta \bar{u})/(u + \bar{u})$ and $(\Delta d + \Delta \bar{d})/(d + \bar{d})$ from HERMES are compared to various parameterizations of the parton distributions.

5 The Future: Strangeness and Gluons

It is obvious that the puzzle about the spin content of the nucleon cannot be understood without measuring the spin distributions of strange quarks and gluons. HERMES has upgraded its spectrometer in 1998 by a dual radiator ring-imaging Čerenkov detector. The aim is to identify kaons in order to be able to tag strange quarks and measure their spin distributions. The chiral field theory, as sketched in Figure 6 describes not only the flavor asymmetry of the sea but it makes also predictions about the quark spin distributions. One interesting prediction is that due to spin flip in the transition $u \to sK^+$,

the positive u-quark polarization produces a negatively polarized strange sea. The anti-strange sea is unpolarized as the K^+, the Goldstone boson in the chiral model, has zero spin[20]. In all experiments up to now the fact that the polarization of quarks and anti-quarks might be different is neglected. By comparing the spin asymmetry in K^+ and K^- production, HERMES has the potential to separate the polarization of the strange sea and anti-strange sea. The separation will however not be easy as the K^+ signal is dominated by a background from up quark fragmentation which has to be subtracted.

From QCD evolution and from the Adler Anomaly we know that the gluon plays an important role for the spin of the nucleon. As gluons have no electromagnetic charge, direct scattering off gluons is not possible by an electromagnetic probe. Only the photon-gluon-fusion process where the virtual photon couples to the gluon by the exchange of a (virtual) quark gives a relatively direct access to the gluon polarization. The cleanest way to measure this process is the identification of two forward jets with large transverse momentum. The experimental separation of jets requires high energies. HERMES currently studies the question if two single hadrons with large transverse momentum are sufficient to isolate photon-gluon-fusion events. A special trigger has been set up at HERMES to enhance the number of high p_T events in photoproduction.

Further channels of photon-gluon-fusion are the open charm and the inelastic J/ψ production. High quality data on the gluon spin are expected from the future project COMPASS[28] at CERN and from Drell-Yan processes at RHIC[29].

6 Conclusions

Semi-inclusive DIS is a rich and important field to study the quark and gluon structure of baryons. The polarized and unpolarized flavor structure of the nucleon has become experimentally accessible. In the interpretation of the data the pionic degree of freedom seems to play an important role. This statement applies to the flavor asymmetry of the light sea, to the spin distributions, and to the high energy leading baryon data at HERA.

7 Acknowledgments

References

1. ZEUS Collaboration, M. Derrick et al., *Phys. Lett.* B **315**, 481 (1993).
2. H1 Collaboration, T. Ahmed et al., *Nucl. Phys.* B **429**, 477 (1994).
3. EMC, M. Arneodo et al., *Z. Phys.* C **36**, 527 (1987).
4. HERMES Collaboration, K. Ackerstaff et al., hep-ex/9806008, accepted by Nucl. Instr. and Meth., (1998).
5. D.P. Barber et al., *Phys. Lett.* B **343**, 436 (1995).
6. R.D. Field and R.P. Feynman, *Phys. Rev.* D **15**, 2590 (1977).
7. R.D. Field and R.P. Feynman, *Phys. Rev.* B **136**, 1 (1978).
8. TASSO, M. Althoff et al., *Z. Phys.* C **22**, 307 (1984).
9. Ph. Geiger, PhD thesis, Univ. Heidelberg, Germany, (1998).
10. E665 Collaboration, M.R. Adams et al., *Z. Phys.* C **76**, 441 (1997).
11. J.J. Van Hunen, Proc. of the Lake Louise Winter Institute for Quantum Chromodynamics, Alberta, Canada, (February 1998).
12. W. Schmidke, contribution to XXIX International Conference on High Energy Physics, Vancouver, Canada, July 23-29, (1998).
13. H1 collaboration, Abstract 569, contribution to XXIX International Conference on High Energy Physics, Vancouver, Canada, July 23-29, (1998).
14. J.M. Niczyporuk, E.E.W. Bruins, *Phys. Rev.* D **58**, 091501 (1998).
15. For a recent review see F.M. Steffens and A.W. Thomas, *Phys. Rev.* C **55**, 900 (1997) and references therein.
16. NMC, M. Arneodo et al., *Phys. Rev.* D **50**, 1 (1994).
17. HERMES Collaboration, K. Ackerstaff et al., hep-ex/9807013, submitted to Phys. Rev. Lett., (1998).
18. E866 Collaboration, E.A. Hawker et al., *Phys. Lett.* B **332**, 244 (1994); E866 Collaboration, J.C. Peng et al., hep-ph/9804288.
19. e.g. A. Szczurek et al., *Nucl. Phys.* A **570**, 765 (1994), A. Szczurek et al., *J. Phys. G.: Nucl. Part. Phys.* **22**, 1741, (1996).
20. E.J. Eichten et al., *Phys. Rev.* D **45**, 2269 (1992); **47**. R747 (1993).
21. EMC, J. Ashman et al., *Phys. Lett.* B **206**, 364 (1988).
22. J. Ellis and M. Karliner, hep-ph/9601280 (1996).
23. SMC, D. Adeva et al., *Phys. Lett.* B **420**, 180 (1998).
24. M.A. Funk, PhD thesis, Univ. Hamburg, (1998); H.A.M. Tallini, PhD thesis, Univ. Liverpool, (1998).
25. J. Bartelski and S. Tartur, *Z. Phys.* C **71**, 595 (1996).
26. T. Gehrmann and W.J. Stirling, *Phys. Rev.* D **53**, 6100 (1996).
27. M. Glück et al., *Phys. Rev.* D **53**, 4775 (1996).
28. COMPASS proposal, CERN/SPSLC-94-14 (March 1996).
29. G. Bunce et al., *Particle World* **3**, 1 (1992).